Scattering of 6–24 MeV Negative Pions by Hydrogen*

ENID BIERMAN†‡
Columbia University, New York, New York
(Received March 5, 1962)

The scattering of negative pions at laboratory energies between 6 and 24 MeV has been observed in a liquid hydrogen bubble chamber. The energy of each scattering was deduced from the ranges and angles of the scattered pion and recoil proton. Flux was measured by direct count of tracks of stopped pions. A maximum likelihood analysis was performed treating the strength of the small P-wave contribution as known. Based on 246 scattering events at a median energy of 13 MeV, the S-wave scattering length $a=(2\alpha_1+\alpha_3)/3\eta$ is found to be 0.090 ± 0.005 when the large Coulomb contribution is assumed to be the nonrelativistic amplitude for pure Coulomb scattering. Results are also presented with further Coulomb corrections. Values of α_1 are computed from the combination of this experimental result with experiments on π^+-p scattering.

I. INTRODUCTION

THE possibility of expressing differential cross sections for all pion-nucleon phenomena in terms of a few parameters has stimulated pion scattering measurements throughout the past decade. In 1953, Fermi[1] developed expressions[2] for the differential cross sections in terms of six phase shifts, under the assumptions that only S and P states are responsible for the scattering and that isotopic spin is conserved. The phase shifts in the S waves are α_1 and α_3 for the isotopic spin states $\frac{1}{2}$ and $\frac{3}{2}$, respectively. The phase shifts in the P waves are $\alpha_{11}, \alpha_{13}, \alpha_{31}, \alpha_{33}$ where the first index denotes twice the isotopic spin and the second index denotes twice the total angular momentum. Fermi also showed[3] that if the interaction can be described by a potential that is zero outside some radius r_0, continuity of the wave function and its derivative requires that the phase shifts in the l state are proportional to η^{2l+1}, as long as ηr_0 is $\ll 1$. η is the momentum of the pion in the center-of-mass system in units of $m_\pi c$, and r_0 is in units of $\hbar/m_\pi c$. To the extent that this analysis is valid, all pion-nucleon interactions are characterized by the six constant amplitudes α_n/η, α_{nm}/η^3. At energies for which constant amplitudes do not adequately fit the data, scattering cross sections have been analyzed in terms of the above six phase shifts without assuming the Fermi momentum dependence.[4]

More recently, there has been renewed interest in these parameters because the difference in the S-wave phase shifts, $\alpha_1-\alpha_3$, was found larger when they were deduced from scattering experiments than when they were deduced from the Panofsky ratio and pion photoproduction. This discrepancy has stimulated theoretical re-examination[5,6] of the low-energy pion phenomena (in particular, extrapolations to zero energy) as well as experimental measurements of improved accuracy.

Two of these recent experiments are the hydrogen bubble chamber measurement of scattering of low-energy positive pions by Fischer and Jenkins[7] and a similar experiment for negative pions that is the subject of this paper. These two experiments can be analyzed to determine the two S-wave phase shifts. In this analysis we take the Coulomb contribution as theoretically given and assume the P-wave phase shifts to be those given by higher energy experiments.

II. EXPERIMENTAL PROCEDURE

A. Exposure

The π^- beam of the Nevis cyclotron was slowed to maximize the number of pions stopping in the 12-in. hydrogen bubble chamber. The dimensions of the chamber-camera system that are involved in analysis of the data of this experiment are shown in Fig. 1. Further details of this chamber have been previously described.[8]

Two cyclotrons runs were used, giving about 13 and 7 stopping pions per picture, respectively, with comparable numbers of nonstopping tracks crossing the picture in each case. There was a magnetic field of 8800 G along the axis of the chamber in each run.

B. Scanning

The film was reprojected one and one-half times original size for scanning and measurement.

Scanners were instructed to consider every three prong event, including those where the shortest prong was so short as to be barely recognizable. They were to

* This work was supported in part by the U. S. Atomic Energy Commission.
† Submitted in partial fulfillment of the requirements for the degree of Doctor of Philosophy in the Faculty of Pure Science, Columbia University.
‡ Present address: Stevens Institute of Technology, Hoboken, New Jersey.
[1] H. L. Anderson, E. Fermi, R. Martin, and D. E. Nagle, Phys. Rev. **91**, 155 (1953).
[2] In reference 1, the cross sections are expressed in terms of intermediate quantities. The differential cross sections are given directly in terms of the phase shifts by J. Ashkin and S. H. Vosko, Phys. Rev. **91**, 1248 (1953).
[3] E. Fermi, Suppl. Nuovo cimento **10**, (1955).
[4] A summary of the experimental values of the phase shifts is Suppl. Nuovo cimento **14**, 221 (1959).
[5] M. Cini, R. Gatto, E. L. Goldwasser, and M. A. Ruderman, Nuovo cimento **10**, 242 (1958).
[6] J. Hamilton and W. S. Woolcock, Phys. Rev. **118**, 291 (1960).
[7] G. E. Fischer and E. W. Jenkins, Phys. Rev. **116**, 749 (1959).
[8] F. Eisler, *et al.*, Nuovo cimento **10**, 468 (1958).

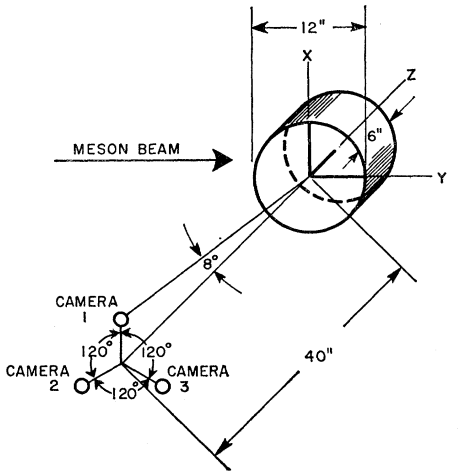

FIG. 1. Schematic view of bubble chamber and cameras, with standard coordinate system.

record all except those for which the projected scattering angle was less than 30° in each view, none of the tracks originated at the edge of the picture, the event was clearly a proton-proton scatter by the reverse curvature of the tracks, or the short, heavy track (proton recoil) was longer than 1.7 cm as remagnified. The requirement that the recoil proton track be visible determined the lower energy limit of the useable events.

60 000 pictures containing about 500 000 flux pions were scanned. About 1000 $\pi^-+p\rightarrow\pi^-+p$ scattering events were examined, of which 246 were used.

A typical event is shown in Fig. 2.

Scanning efficiency was measured, and maintained at almost 100%, by double and triple scanning in different views. 50% of the film was scanned by three different scanners using the two clearest views, or by one scanner separately in each of two views, and another scanner in the clearer of those views. 45% of the film was scanned in two different views by two different scanners. In this case, the two scanners were among the most efficient.

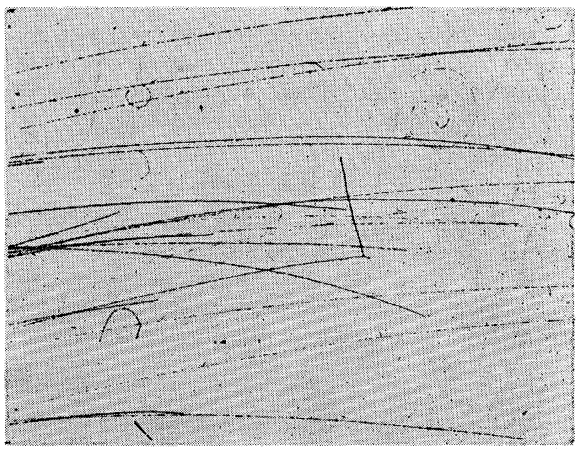

FIG. 2. Typical event. $E_{\text{lab}}=13.3$ MeV; $\theta_{\text{c.m.}}=108°$.

The remaining 5% was scanned by one scanner in two different views.

C. Measurements

A fiducial region was chosen to exclude the edges of the chamber. This was done for the sake of scanning efficiency, picture quality, and to reduce the fraction of events in which the scattered pion left the chamber. It also precluded confusion between tracks that left the face of the chamber and genuine flux tracks that ended barely within the chamber. The fiducial region constituted 45% of the chamber volume.

For each event, the path length from the interaction point to the far side of the fiducial circle was measured. This was compared with the range corresponding to the energy at which the interaction took place, and only those scatterings were used for which the pion would have stopped within the fiducial circle. In depth, the corresponding check was made by computing the depth z where the incoming pion would have stopped had it not scattered. This z is the z of the interaction plus the range corresponding to the energy at which the scattering occurred times the z direction cosine. The event was used only if this computed z was 1.3 cm or more within the chamber.

Events were measured in each of three views. Angles with respect to the scanning table were measured for the incoming pion, scattered pion, and recoil proton. Projected lengths of the outgoing pion and proton were measured. To measure the projected coordinates of the point of interaction, a transparent Cartesian grid was aligned with three reference marks that appeared in each picture.

In order to avoid extensive work on scatterings that were primarily due to the Coulomb interaction, events were not measured if their projected scattering angle was less than 50° in every view. This eliminated a calculated fraction of the scatterings within the desired range of scattering angles; however, the eliminated ones were only ones seen close to "edge on" and these were not used for other reasons, as discussed below. This effect is referred to as "forward angle bias" in the discussion of efficiency below.

Measurements in the three projected views were converted into true three-dimensional quantities with the aid of an IBM 650 computer.

First coordinates and angles were transformed to a standard coordinate system as in Fig. 1. This system has its origin at the center of the inside front face of the chamber. The x-y plane is the plane of the pictures. z is into the chamber along the chamber axis. Thus, the inside back face is the plane $z=15$ cm. The beam traveled roughly along the y axis.

After projected measurements were transformed to the standard coordinate system, the following quantities were calculated: x, y, z of the event; direction cosines of incoming and outgoing pions and recoil

proton; φ_{lab}; θ_{lab}; $\theta_{c.m.}$ (from pion measurements); $180°-2\varphi_{lab}$, which is $\theta_{c.m.}$ from proton angle measurements; and ranges of outgoing pion and proton.

The final step performed by the computer was calculation of the uncertainties on the angle of each track with respect to the z axis, and the uncertainties on the lengths. This was possible because measurement in the third view made each angle and length overdetermined.

D. Energy and Angle Determination

The energy and angle of each scattering were determined from the angles and ranges of the outgoing particles. The curvature of the incoming track would have given a much poorer determination of energy.

An event is completely determined by one range and one angle, or two ranges. When more than two of these quantities were measured, the data were all taken into account with rough weighting being given according to their errors of measurement. Proton length and pion angle measurements were always available. Pion length was unavailable if the scattered pion left the chamber, and proton angle was unmeasurable if the proton was so slow that its track length was comparable to track width.

Occasionally the separate data did not agree as well as expected, or the errors indicated that the three views did not agree as well as expected. Such cases were remeasured with extra care. These inaccuracies did not constitute a significant difficulty.

E. Azimuthal Distribution and Scanning Efficiency

Evaluation of the efficiency made it essential to consider the relation between the plane containing the three particle tracks (the scattering plane) and the plane of the pictures (the x-y plane). We define three angles, shown in Fig. 3.

Azimuth ϕ. The angle between the scattering plane and the line in the x-y plane which is perpendicular to the incident pion track.

Dip. The angle between the scattering plane and the x-y plane.

Inclination α. The angle between the incident pion's track and the x-y plane.

Note that when $\phi=0$, dip$=\alpha$. The true scattering is independent of azimuth.

For all scattering events the inclination α of the incident pion at the point of scattering was plotted. The distribution was centered 1.4° from the x-y plane, was Gaussian shaped, and had a half width of 7.5°. Since it was so close to centered on the x-y plane, the rms value of the inclination was also approximately 7.5°. For this distribution of incident pions the aximuth of the event is approximately the same as the dip, except when the plane of the scattering is within about 15° of the x-y plane. Dip was computed for each event, using the direction cosines of incoming and outgoing pions; azimuth was computed from $\cos\phi=\cos(\text{dip})/\cos\alpha$.

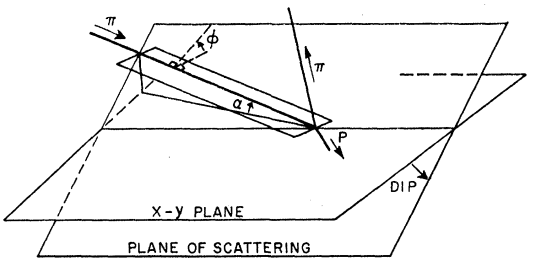

FIG. 3. Angles involved in efficiency evaluation. The x-y plane is parallel to the chamber faces and to the film. The angle between incident pion and x-y plane is inclination α. ϕ is azimuth angle. $\phi\approx$ dip except when $\phi\approx0$. Events having dip$\approx90°$ appeared distorted and were frequently missed.

Some inefficiency was expected in scanning for or identifying "edge on" events; i.e., those near 90° of dip, due to their distorted appearance. For instance, backward μ-e decays and pion-proton scatterings appear similar when seen edge on, if the electron or outgoing pion leaves the chamber face.

The azimuthal distribution of events, with and without correction for the forward angle bias, is shown in Fig. 4. The falling off in abundance of edge on events, for the corrected distribution, is attributed to missed or misinterpreted events.

There are two other indications of edge-on inefficiency. The shaded events in Fig. 4 are those for which the measurer had doubts that the event was genuine. This phenomenon is seen to be strongly correlated with dip. The other indication is the decreasing single-

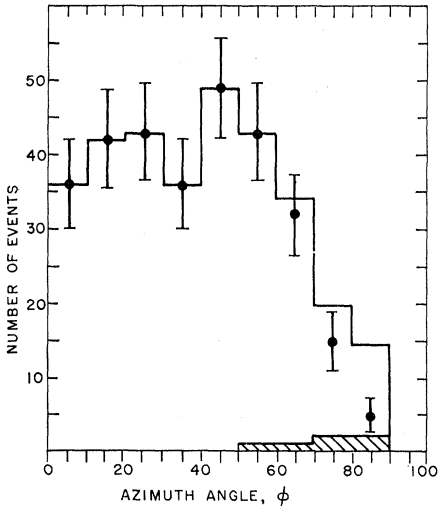

FIG. 4. Azimuthal distribution of events. Points show number of events found. Histogram includes correction for bias introduced by projected angle criterion. Lack of "edge on" events, $\phi=60°$ to 90°, indicates that this portion of data is unreliable.

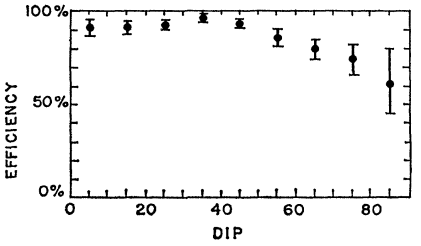

FIG. 5. Average single-scanner scanning efficiency.

scanner efficiency in picking up the events of large dip, as displayed in Fig. 5.

On the basis of the evidence of Figs. 4 and 5, it was decided that the most reliable measurement of the desired scattering length would be one based on the events within 60° of the x-y plane. There are 246 such events. They are unbiased by any criterion.

For these events the single-scanner scanning efficiency averaged 92%. Assuming that misses are uncorrelated from one scanner to another (the experiment showed no evidence against this), and that different scanners have the same efficiency, (quite far from true) double scanning leaves 0.6% of the events missed, and triple scanning 0.05% missed. These losses are so small as to make more rigorous analysis of efficiency superfluous. Considering that correlation would raise the loss, different individual efficiencies lower it, and that the statistical knowledge of the missed events is quite limited, the efficiency for finding the events is estimated at $99\%+1\%,-2\%$. There appeared no correlation of misses with energy or angle.

The 246 scattering events used are therefore 99% of those that satisfy all of the following:

(1) The incoming pion had energy in the lab$\geq$6 MeV when it scattered;

(2) It scattered at a center-of-mass angle$>$99° if $E=6$ to 10 MeV, $>$65° if $E>10$ MeV;

(3) The plane of the event was within 60° of the plane of the pictures;

(4) The pion would have stopped in the fiducial region had it not scattered.

Energies and angles of the events are shown in Fig. 6.

F. Flux Measurement

The probability of observing a scattering event at an energy corresponding to range R is proportional to the number of flux pions $N(R)$ that existed at this range R. Letting R_m be the range from where the track entered the fiducial region to where it stopped, $N(R)$ is the number of tracks for which $R_m>R$. This is shown in Fig. 7.

To determine $N(R)$ it was necessary to measure the ranges R_m of a sample of tracks, and to determine the total number of flux tracks.

The number of stopping pions was counted in every 100th picture. Due to the slightly different remagnifications in the three views, precise determination of depth z for each ending would have required computation involving x and y. Since all that was required was that the fiducial region be consistent for the scatterings and the flux, it was most efficient to use a criterion giving only an average correct z. This criterion was that the remagnified positions of the flux track ending should differ in two views by 0.45 to 4.50 cm. This corresponds to the region 1.3 cm or more from either face of the chamber.

The energy distribution of the flux was measured by measuring the range of each flux track in every second flux-counted picture. The remagnified range was converted to true range using the factor correct for the peak in z of the flux distribution. Due to the differently chosen fiducial region, this procedure did not require the correction in magnification for long tracks that was made in the experiment of Fischer and Jenkins.

The only flux count correction was that due to decay of pions in flight. The decays in flight were not counted because of the extra measurements and computations necessary to determine their energy. Instead, the fraction of the pions existing at energy E that would have decayed in flight at energies between E and zero was calculated from the pion lifetime. The measured flux at E was then augmented by this amount to obtain the total scatterable flux. The correction increases with energy, reaching 6.6% at 24 MeV.

III. CALCULATION OF THE SCATTERING LENGTH

If one assumes that only S and P states contribute to the scattering, and assumes charge independence, then the differential cross section for elastic $\pi^- - p$ scattering in the center of mass is related to the phase shifts by

$$\frac{d\sigma}{d\Omega}=\frac{1}{36k^2}[|e^{2i\alpha_3}+2e^{2i\alpha_1}-3+(2e^{2i\alpha_{33}}+e^{2i\alpha_{31}}+4e^{2i\alpha_{13}}+2e^{2i\alpha_{11}}-9)\cos\theta|^2+|(e^{2i\alpha_{33}}-e^{2i\alpha_{31}}+2e^{2i\alpha_{13}}-2e^{2i\alpha_{11}})\sin\theta|^2].$$

This is modified for low energies by letting $\sin\alpha\to\alpha$ and including the Coulomb amplitude nonrelativistically,

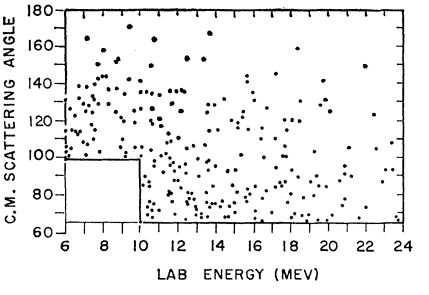

FIG. 6. Energies and angles of the 246 events used in experiment.

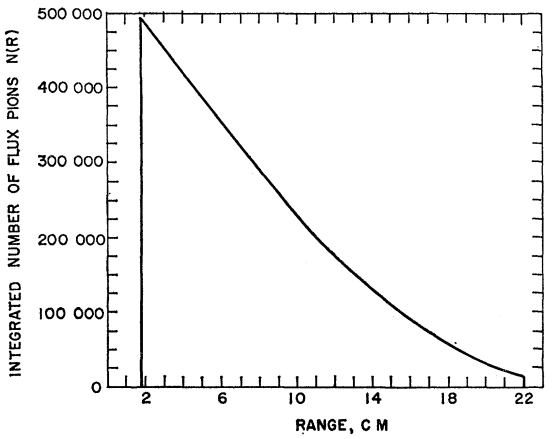

FIG. 7. Flux distribution. $N(R)$ is the number of pions that traversed a distance greater than R in all pictures scanned. The probability of observing a scattering at an energy E corresponding to a range R is $N(R)$ times the probability that a single pion will scatter at E.

resulting in[9]

$$\frac{d\sigma}{d\Omega}=\lambda\!\!\!^{-}_c{}^2\left|\left(\frac{2\alpha_1+\alpha_3}{3\eta}+\frac{2\alpha_{33}+\alpha_{31}+4\alpha_{13}+2\alpha_{11}}{3\eta}\cos\theta\right.\right.$$
$$\left.\left.+\frac{e^2}{\hbar v\eta(1-\cos\theta)}\right)^2+\left(\frac{(\alpha_{33}-\alpha_{31}+2(\alpha_{13}-\alpha_{11})}{3\eta}\sin\theta\right)^2\right|, \quad (1)$$

where $\lambda\!\!\!^{-}_c=\hbar/m_\pi c$=reduced Compton wavelength of the pion; $\eta=\hbar k/m_\pi c$=pion's center-of-mass momentum in units of $m_\pi c$. $\lambda\!\!\!^{-}_c{}^2/\hbar v\eta(1-\cos\theta)$ is the amplitude for Coulomb scattering. v is the relative velocity of the pion and proton. The validity of including the Coulomb scattering only nonrelativistically is established by Solmitz.[10]

The S-wave scattering length $a=(2\alpha_1+\alpha_3)/3\eta$ is calculated from the data of this experiment by the maximum likelihood method. The P-wave phase shifts are taken to be $\alpha_{33}=0.22\eta^3$, all others zero. a is so insensitive to the assumed value of α_{33} due to the low energy of this experiment that a change of α_{33} by the variation of recently reported values[4,11] $0.024\eta^3$, changes a by only 0.3%. However, the uncertainties in α_{13} and α_{11} are not negligible compared to the other errors in the present experiment. Barnes *et al.*[11] find $\alpha_{31}/\eta^3=-0.042\pm0.004$, $\alpha_{13}/\eta^3=-0.055\pm0.062$, $\alpha_{11}/\eta^3=-0.016\pm0.11$. Using these values would lower a by 2%. Using these values stretched to the limits of their errors. $\alpha_{31}/\eta^3=-0.05$, $\alpha_{13}/\eta^3=-0.12$, $\alpha_{11}/\eta^3=-0.13$, would lower a by 5%.

The density of hydrogen was 0.0565±0.0005 g/cc as determined for this bubble chamber by the measurement of ranges of muons from pion decay.[12]

Following Fischer and Jenkins, the probability of finding an event in this experiment within an angular interval $\Delta x_i=2\pi\sin\theta_i\Delta\theta_i$ and an energy interval ΔE_i is

$$\left(\frac{d\sigma}{d\Omega}\right)_i N(E_i)\frac{\text{density of hydrogen}}{\text{mass of } H \text{ atom}}\frac{dR}{dE}\Delta E_i\Delta x_i,$$

where $N(E_i)$ is the number of flux tracks that existed with energy E_i in all film scanned, and R is the range of a pion of energy E. The probability of not finding an event is one minus the previous expression. The probability that the experiment would give just N events occurring at x_i, E_i is the probability for finding N events in the intervals Δx_i, ΔE_i times the probability of not finding any events in all other intervals.

$$L=\left\{\prod_{i=1}^{N}\left(\frac{d\sigma}{d\Omega}\right)_i N(E_i)\frac{\rho_H}{m_H}\Delta R_i\Delta x_i\right\}$$
$$\times\left\{\prod_{j\neq i}\left[1-\left(\frac{d\sigma}{d\Omega}\right)_j N(E_j)\frac{\rho_H}{m_H}\Delta R_j\Delta x_j\right]\right\},$$

which in the limit of small intervals becomes

$$L=\left\{\prod_{i=1}^{N}\left(\frac{d\sigma}{d\Omega}\right)_i N(E_i)\frac{\rho_H}{m_H}dR_i dx_i\right\}$$
$$\times\left\{\exp\left(-\frac{\rho_H}{m_H}\int\int\frac{d\sigma}{d\Omega}N(R)dRdx\right)\right\}.$$

It is more convenient to work with the logarithm of the likelihood. Performing the angular integration and dropping constant terms,

$$\ln L=\sum_{i=1}^{N}\ln\left(\frac{d\sigma}{d\Omega}\right)_i-\frac{\rho_H}{m_H}\int\sigma(R)N(R)dR,$$

where σ is the total cross section for the angular interval used. Putting in the limits of this experiment,

$$\ln L=\sum_{i=1}^{246}\ln\left(\frac{d\sigma}{d\Omega}\right)_i-\frac{\rho_H}{m_H}\int_{1.80\text{cm}}^{4.6\text{cm}}\sigma_1(R)N(R)dR$$
$$-\frac{\rho_H}{m_H}\int_{4.6\text{cm}}^{22.0\text{cm}}\sigma_2(R)N(R)dR,$$

where

$$\sigma_1=\int_0^{60°}4d\phi\int_{99°}^{180°}\frac{d\sigma}{d\Omega}\sin\theta d\theta$$

and

$$\sigma_2=\int_0^{60°}4d\phi\int_{65°}^{180°}\frac{d\sigma}{d\Omega}\sin\theta d\theta.$$

[9] H. A. Bethe and F. de Hoffmann, *Mesons and Fields* (Row, Peterson and Company, Evanston, Illinois, 1955), p. 82.
[10] F. T. Solmitz, Phys. Rev. **94**, 1799 (1954).
[11] S. W. Barnes, B. Rose, G. Giacomelli, J. Ring, K. Miyake, and K. Kinsey, Phys. Rev. **117**, 226 (1960); and S. W. Barnes, H. Winick, K. Miyake, and K. Kinsey, *ibid.* **117**, 238 (1960).
[12] R. J. Plano, Phys. Rev. **119**, 1400 (1960).

TABLE I. Scattering length $a=(2\alpha_1+\alpha_3)/3\eta$ deduced from the data of this experiment.

	Raw, Eq. 1	With outer Coulomb corrections		With inner and outer Coulomb corrections	
		$r_0=0.5\lambda\!\!\!^{-}_c$	$r_0=\lambda\!\!\!^{-}_c$	$r_0=0.5\lambda\!\!\!^{-}_c$	$r_0=\lambda\!\!\!^{-}_c$
a	0.090 ± 0.005	0.088	0.094	0.087	0.087

This was evaluated with a desk calculator for $a=0.086$, 0.090, and 0.094. It was checked in two ways: the contribution of each event was compared for the three values of a to find any irregularity, and each event was entered on an E vs $\ln(d\sigma/d\Omega)$ plot and contour lines of θ drawn to find any irregularity.

A parabola was fitted to the three values of $\ln L$. The "raw scattering length" given in Table I is the value of a for which $\ln L$ is a maximum. The half width of the parabola where $\ln L$ has dropped from its maximum by 0.5 is 0.0034. This is the error on a due only to the statistical uncertainty in the number of events. Other errors considered were uncertainty of scanning efficiency, identification of odd-looking events, human inconsistency in flux counting and range measurement, precision of energy and angle determination for each event, statistics on $N(E)$, and the accuracy of hydrogen density. Each of these errors is one fourth or less of the statistical error on the number of scattering events. The error quoted in Table I is the combined effect of the statistical error and these other errors. The uncertainty due to α_{13} and α_{11} is not included.

When the likelihood calculation was carried out for four separate energy intervals, no consistent or statistically significant variation in a was found.

IV. RESULTS AND DISCUSSION

A. Further Coulomb Effects

The effect of the Coulomb potential is not fully described by the pure Coulomb term in the raw scattering length expression, Eq. 1. In other words, the a in this expression is not purely a measure of the nuclear interaction. Assuming the nuclear interaction extends to a radius r_0, the additional effect due to the existence of the Coulomb potential at $r>r_0$ has been calculated by Van Hove,[13] and that due to the Coulomb potential at $r<r_0$ has been calculated by Hamilton and Woolcock.[6] Following Hamilton and Woolcock, the former is designated as the outer Coulomb correction, and the latter as the inner Coulomb correction. An outer-corrected phase shift is significantly dependent on the value used for r_0, but the complete correction removes most of this dependence.

The corrections were performed separately for the $T=\frac{3}{2}$ and $T=\frac{1}{2}$ phase shifts and then combined according to $\Delta a=(2\Delta\alpha_1+\Delta\alpha_3)/3\eta$. To permit comparison with other experiments the corrections were computed for $r_0=\hbar/m_\pi c=1.40\times10^{-13}$cm, the pion's reduced compton wavelength, and for $r_0=0.70\times10^{-13}$cm which is the radius indicated by the electron scattering measurements of Chambers and Hofstadter.[14] The various values are shown in Table I. Of these $a=(2\alpha_1+\alpha_3)/3\eta=0.087\pm0.005$ should best describe the purely nuclear S-wave π^--p elastic scattering.

B. Comparison with other π^- Scattering Experiments

The earliest bubble chamber measurement of low-energy π^--p scattering was made by Nagle, Hildebrand, and Plano[15] in 1956. Their result was determined primarily by 27 events for which the pion would have stopped in the chamber had it not scattered. They found a scattering length $a=(2\alpha_1+\alpha_3)/3\eta=0.077\pm0.011$ which is not in disagreement with the present experiment.

No other experiments have been performed at energies below 30 MeV.

Barnes *et al.*[11] have performed an extensive series of counter measurements of $\pi^\pm$ scattering from 30 to 150 MeV. They find $\alpha_1/\eta=0.205\pm0.005$, $\alpha_3/\eta=-0.115\pm0.003$, where the statistical errors are estimates by Hamilton and Woolcock.[6] Using a different method of analysis, Hamilton and Woolcock find $\alpha_1/\eta=0.178\pm0.005$, $\alpha_3/\eta=-0.087\pm0.005$. These analyses imply $a=0.098$ and 0.090, respectively. The Barnes values are inconsistent with the Panofsky ratio and photoproduction; the Hamilton and Woolcock values indicate consistency among the parameters. It is clear that comparison of the present experimental result ($a=0.087\pm0.005$) with higher energy counter experiments depends more on the method of extrapolation than on the measured values of the cross sections.

C. Relation to π^+ Scattering

To the extent that the $T=\frac{3}{2}$ S-wave phase shift α_3 is known, this experiment determines the $T=\frac{1}{2}$ S-wave phase shift α_1 by $\alpha_1/\eta=(3a-\alpha_3/\eta)/2$.

The $\pi^++p\to\pi^++p$ experiment of Fischer and Jenkins gives $\alpha_3/\eta=-0.104\pm0.006$. This includes the "outer" correction using $r_0=0.5\lambda\!\!\!^{-}_c$. Combining it with the similarly corrected π^- scattering length from the present experiment, $\alpha_1/\eta=0.184$. Correcting this α_3/η by the inner Coulomb correction as well makes it $\alpha_3/\eta=-0.103$, which when combined with the correspondingly corrected a gives $\alpha_1/\eta=0.182$.

Hamilton and Woolcock consider the best value to be $\alpha_3/\eta=-0.087\pm0.005$. This is based on the Fischer and Jenkins experiment and higher energy experiments

[13] L. Van Hove, Phys. Rev. **88**, 1358 (1952).

[14] E. E. Chambers and R. Hofstadter, Phys. Rev. **103**, 1454 (1956).

[15] D. E. Nagle, R. H. Hildebrand, and R. J. Plano, Phys. Rev. **105**, 718 (1957).

fitted to a theoretical relation.[16] It contains an outer Coulomb correction using $r_0=\lambda\!\!\!^{-}_c$. This value for α_3/η and the present experimental a give $\alpha_1/\eta=0.184$. The same α_3/η and a, except using $r_0=0.5\lambda\!\!\!^{-}_c$, give $\alpha_1/\eta=0.174$. If we now apply the inner Coulomb correction as well, we get $\alpha_1/\eta=0.170$ and 0.172 using $r_0=\lambda\!\!\!^{-}_c$ and $0.5\lambda\!\!\!^{-}_c$, respectively.

The Hamilton and Woolcock analysis gives $\alpha_1/\eta=0.178\pm0.005$ with outer Coulomb correction using $r_0=\lambda\!\!\!^{-}_c$. The comparable value found from this experiment is $\alpha_1/\eta=0.184$ using the α_3/η of Hamilton and Woolcock. The present experiment is therefore not in disagreement with the consistent low-energy pion parameters of Hamilton and Woolcock.

[16] The value of α_3/η preferred by Hamilton and Woolcock is not directly comparable with that reported by Fischer and Jenkins. When the Fischer and Jenkins result is corrected using $r_0=\lambda\!\!\!^{-}_c$, it becomes $\alpha_3/\eta=-0.108$. Furthermore, the Fischer and Jenkins amplitude fell off at low energies by $1\frac{1}{2}$ standard deviations.

V. ACKNOWLEDGMENTS

The author wishes to thank Professor Jack Steinberger for suggesting this experiment and for continued guidance. The entire Columbia Bubble Chamber group carried out the exposure. The conscientious work of many scanners is appreciated, notably Irene Garder, Alex Rytov, and Mary Johnson, and the careful measurements and analysis by Herman Kaufman. The author also thanks Dr. Daniel Tycko for assistance in the use of the IBM 650.

Special appreciation is expressed to Dr. Edgar Jenkins and Dr. Gerhard Fischer for discussions of their similar experiment at the outset of this experiment

PHYSICAL REVIEW VOLUME 127, NUMBER 2 JULY 15, 1962

Probable Example of the Decay $\Sigma^0\to\Lambda+e^+e^-$ in Nuclear Emulsion

D. H. DAVIS,* R. LEVI SETTI, M. RAYMUND, AND G. TOMASINI†
The Enrico Fermi Institute for Nuclear Studies,‡ The University of Chicago, Chicago, Illinois
(Received March 15, 1962)

An event has been observed in nuclear emulsion which is attributed to the production of a Σ^0 hyperon and its subsequent decays via the mode $\Sigma^0\to\Lambda+e^+e^-$. From the apparent concurrence of the tracks involved in the disintegrations, it has been deduced that the Σ^0 lifetime for this event is $<10^{-14}$ sec.

THE lifetime of the Σ^0 hyperon is expected to be within the range 10^{-18}–10^{-20} sec,[1,2] and possible methods for its determination have been recently discussed by Dreitlein and Primakoff.[3] Until now the sole experimental value reported[4] was obtained from the observation of Σ^0 hyperon decay events in a hydrogen bubble chamber by Alvarez *et al.*[5] The Σ^0 hyperon lifetime was quoted to be less than 10^{-11} sec. During the systematic scanning for K^- meson captures at rest in an Ilford $K5$ emulsion stack an event has been found which is attributed to the decay of a Σ^0 hyperon via the Dalitz mode, i.e.,

$$\Sigma^0\to\Lambda^0+e^+e^-. \qquad (1)$$

This decay mode was first observed by Eisler *et al.*[6] in a hydrogen bubble chamber. The high spatial resolution of the emulsion technique has enabled a much more precise experimental upper limit to be placed upon the decay length and hence the lifetime of the Σ^0 hyperon.

A photograph of the event to be described is shown in Fig. 1 and the measurements made on it are summarized in Table I. A K^- meson is captured at point O and three fast charged particles are seen to be emitted from the resulting nuclear disintegration. One is due to a charged π meson, probably negative, because it interacts in flight after a path length of 9.1 mm to form a star from which no charged secondaries are emitted. The energy of this π meson, as determined by ionization and scatter-

TABLE I. Summary of the measurements.

Track	φ (deg)	λ (deg)	Observed length (μ)	g^*	$p\beta$ MeV/c	Kinetic energy (MeV)
e_1	184.8	+10.6	2200	0.96±.04	28± 9	28± 9
e_2	187.7	+ 5.7	3300	1.07±.03	48±10	48±10
$\pi^\pm$	45.3	+16.2	9100	1.28±.02	90±17	57± 4

* Fulbright Travel Scholar on leave from University College London.

† On leave of absence from the University of Genoa.

‡ Work supported by the U. S. Air Force Office of Scientific Research, Contract AF 49(638)-209.

[1] M. Gell-Mann and A. H. Rosenfeld, Ann. Rev. Nuclear Sci. **7**, 407 (1957).

[2] J. Dreitlein and B. Lee, Phys. Rev. **124**, 1274 (1961).

[3] J. Dreitlein and H. Primakoff (to be published).

[4] W. H. Barkas and A. H. Rosenfeld, University of California Radiation Laboratory Report UCRL-8030, 1961 (unpublished), revised.

[5] L. W. Alvarez, H. Bradner, P. Falk-Vairant, J. D. Gow, A. H. Rosenfeld, F. T. Solmitz, and R. D. Tripp, University of California Radiation Laboratory Report UCRL-3775, 1957 (unpublished).

[6] F. Eisler, R. Plano, N. Samios, J. Steinberger, and M. Schwartz, Phys. Rev. **110**, 226 (1958).

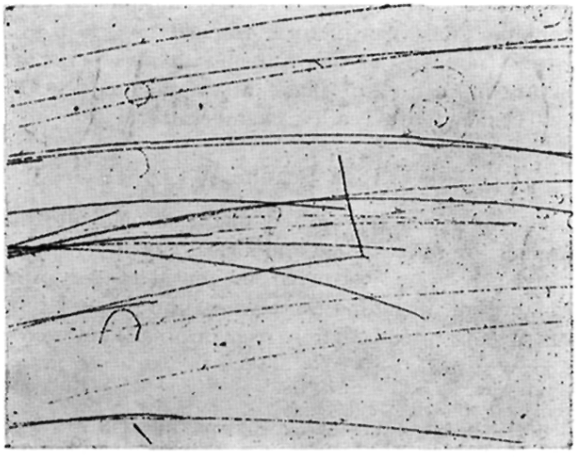

FIG. 2. Typical event. $E_{\text{lab}}=13.3$ MeV; $\theta_{\text{c.m.}}=108°$.